

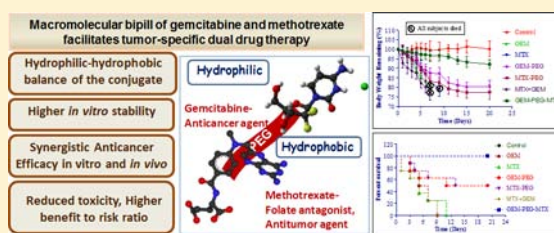
## Macromolecular Bipill of Gemcitabine and Methotrexate Facilitates Tumor-Specific Dual Drug Therapy with Higher Benefit-to-Risk Ratio

Manasmita Das, Roopal Jain, Ashish Kumar Agrawal, Kaushik Thanki, and Sanyog Jain\*

Centre for Pharmaceutical Nanotechnology, Department of Pharmaceutics, National Institute of Pharmaceutical Education and Research (NIPER), Sector 67, S.A.S. Nagar (Mohali), Punjab 160062, India

### S Supporting Information

**ABSTRACT:** The present study reports the synthesis, characterization, and biological evaluation of a novel macromolecular bipill, synthesized by appending two different anticancer agents, viz., gemcitabine (GEM) and methotrexate (MTX), to the distal ends of a long-circulating poly(ethylene glycol) (PEG) spacer. Covalent conjugation of GEM and MTX via PEG linker not only transformed the solubility profiles of constituent drug molecules, but significantly improved their stability in the presence of plasma. *In vitro* cytotoxicity studies confirmed that GEM-PEG-MTX exerts higher cytotoxicity ( $IC_{50}$  0.181  $\mu$ M at 24 h) in human breast adenocarcinoma MCF-7 cell lines, when compared to free drug congeners, i.e., free GEM ( $IC_{50}$  0.294  $\mu$ M at 24 h) and free MTX ( $IC_{50}$  0.591  $\mu$ M at 24 h). Tumor growth inhibition studies in chemically induced breast cancer bearing rats established the superiority of GEM-PEG-MTX conjugate over all other pharmaceutical preparations including free drugs, physical mixture of GEM and MTX, and PEGylated GEM/MTX. Toxicity studies in tumor bearing rats as well as healthy mice corroborated that dual drug conjugation is an effective means to synergize the therapeutic indices of potential drug candidates while alleviating drug-associated side effects.



### INTRODUCTION

Combination therapy may be regarded as one of the most powerful strategies to obviate the compensatory mechanisms and undesired off-target effects that detract the therapeutic utility of potential drug candidates.<sup>1,2</sup> Synergistic combination of two or more therapeutically relevant molecules is known to alleviate the deleterious side effects associated with high doses of single drug molecule by counteracting biological compensation and reducing the dosage of each compound while maximizing their therapeutic effects. Although combination or polypill approach has shown promise in the clinical regimen, each drug molecule in a particular combination has its own unique pharmacokinetic and dynamic profile. Consequently, synchronizing and unifying the pharmacokinetics, on-target accumulation, and intracellular uptake of various drug molecules poses one of the most critical challenges of this therapeutic strategy. Therefore, these limitations need to be surmounted in order to enable precise control of the dosage and scheduling of the multiple drugs for maximal exploitation of combinatorial effects.

To date, a myriad of nanocarrier-based systems based on polymeric nanoparticles or liposomes have been used to codeliver multiple drug molecules to their site of action. While many of them have shown promise in the context of synergistic enhancement of therapeutic effects, fine control of the comparative loading yield and release kinetics of multiple drug payloads on a single system is yet to take shape. In this regard, it will be particularly beneficial if two or more drug molecules are chemically conjugated to each other via

intracellularly hydrolyzable linkers that allow the therapeutic activity of each constituent drug to be resumed following their delivery into their target cells. Since combinatorial conjugation of two or more drug molecules leads to the formation of a new drug entity, it holds tremendous potential to circumvent the major solubility and/or pharmacokinetic-related problems associated with the constituent drug molecules while bestowing an array of beneficial properties and functions that are crucial for synergism. Despite these positive attributes, combinatorial conjugates are still in the very nascent stage of their development. So far, there is only one report in which a combinatorial conjugate of two anticancer drugs, Gemcitabine and Paclitaxel, was synthesized and examined for its time dependent hydrolysis kinetics and cytotoxicity against human pancreatic cell line.<sup>3</sup> Although the synthesized conjugate presented higher *in vitro* cytotoxicity than its free drug congeners, this article does not address whether the combinatorial conjugation strategy works *in vivo* as well. Considering the lacuna of the existing report, we sought to examine whether combinatorial conjugation strategy can be used as a toolbox to synergize the therapeutic indices of clinically established drug molecules with poor biopharmaceutical properties.

The present study reports the synthesis, characterization, and *in vivo* evaluation of a novel macromolecular bipill, constituted

Received: October 17, 2013

Revised: February 9, 2014

Published: February 10, 2014



of two different anticancer agents: methotrexate (MTX) and gemcitabine (GEM). Notable, primary clinical reports have illuminated the feasibility of using a combination of the folate antagonist MTX and nucleoside analogue, GEM, for (i) effective, second-line treatment of patients suffering from relapsing and/or metastatic head and neck cancer (HNC)<sup>4</sup> and (ii) regression of malignant pleural mesothelioma (MPM).<sup>5</sup> Ironically, both these drug molecules have been reported to present severe pharmacokinetic problems. As documented in various primary<sup>6–10</sup> and secondary<sup>11,12</sup> studies, GEM is a highly hydrophilic (solubility ~83 mg/mL) anticancer agent with very short plasma half-life (~45 min). Furthermore, it is prone to rapid clearance from the body through renal excretion upon enzymatic (cytidine-deaminase) conversion to an inactive and more soluble metabolite 2',2'-difluorodeoxyuridine (dFdU) expressed in blood, liver, kidney, and various tumor tissues. Consequently, frequent administration scheduled at high doses is required, thereby leading to myelosuppression and high levels of hepato- and nephrotoxicity.<sup>13</sup> On the other hand, anticancer efficacy of MTX is severely compromised by its toxic, dose-related side effects, closely related to its poor pharmacokinetics. In some earlier studies from our group, we have used magnetic nanoparticle,<sup>14</sup> albumin nanoparticle,<sup>15</sup> and carbon nanotube<sup>16</sup> based multifunctional nanosystems to augment the targeting and therapeutic index of MTX. Apart from nanocarrier-based approaches, PEGylation has been widely used to improve the targeting indices of drug molecules, presenting pharmacokinetic (PK) and metabolic challenges. In a number of studies, MTX and GEM have been separately PEGylated and the resultant bioconjugates have shown improved PK profile *in vivo*.<sup>13</sup> We hypothesized that covalent appendage of GEM and MTX to the distal ends of a heterobifunctional PEG spacer will produce a new, macromolecular bipill, which, by virtue of its improved biopharmaceutical properties, will present synergistic therapeutic responses as compared to its free drug counterparts or single, PEGylated congeners.

## MATERIALS AND METHODS

**Materials and Reagents.** GEM and MTX were provided as gift sample from Fresenius Kabi Oncology Limited, Gurgaon, India. O-(2-Aminoethyl)-O'-(2-carboxymethyl) polyethylene 3500 hydrochloride (NH<sub>2</sub>-PEG-COOH) and O-[(N-succinimidyl) succinyl-aminoethyl]-O'-methylpolyethylene glycol (m-PEG-NHS) were purchased from JenKem Technology, USA. Succinic anhydride, anhydrous solvents (dimethyl sulfoxide, dimethyl formamide, and benzene) and dialysis membrane (1000 KD MWCO) were procured from Sigma Aldrich, USA. Pyridine, dichloromethane, and diethyl ether were purchased from Merck, while dicyclohexylcarbodiimide (DCC) and N-hydroxysuccinimide (NHS) were purchased from Fluka. Sodium bicarbonate, disodium hydrogen phosphate, and sodium acetate were purchased from Loba Chemie Pvt. Ltd., Mumbai. Dichloromethane and pyridine were dehydrated over phosphorus pentoxide and potassium hydroxide, respectively, and distilled prior to use. All other solvents and reagents, unless otherwise stated, were of analytical grade and procured from local suppliers.

**Synthesis and Spectral Characterization of GEM-Bioconjugate (GEM-PEG-MTX).** *General.* The synthesis of GEM-PEG-MTX conjugates is detailed in three steps shown in Figure 1. These steps included: (i) preparation of active NHS ester of MTX using standard carbodiimide chemistry; (ii) PEGylation of the activated ester; and (iii) covalent conjugation

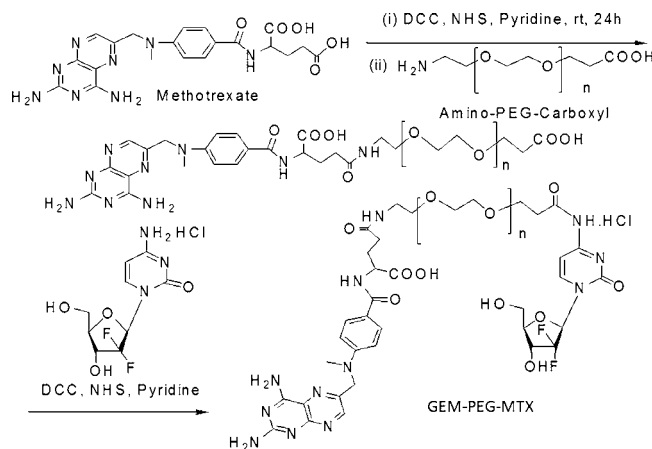


**Figure 1.** Schematic illustration depicting the synthesis of GEM-PEG-MTX conjugate.

of activated ester of PEG-derived MTX with GEM HCl. The chemical structures of target construct and intermediates were authenticated using complementary spectroscopic tools, viz., UV, FTIR, NMR, and mass spectroscopy. UV analysis (Shimadzu UV 1800) was carried out by dissolving 1 mg of conjugate in 1 mL of deionized water and scanning in the range of 200 to 600 nm. The FTIR (Perkin-Elmer, FTIR spectrometer, USA) spectra were recorded using KBr pellet method over a range of 4400–400 cm<sup>-1</sup>. The chemical structure of GEM-PEG-MTX was authenticated via proton (<sup>1</sup>H) NMR analysis by dissolving conjugate in DMSO-*d*<sub>6</sub> (99.9 atom % deuterium-enriched, Sigma-Aldrich Inc., USA) with 0.1% TMS as an internal reference. The NMR analysis was done using Bruker BioSpin (Fallanden, Switzerland) Avance III 400 MHz NMR spectrometer (9.4 T, 54 nm vertical-bore magnet) equipped with a 5 mm BBFO-Plus multinuclear probehead with Z-Gradient, operating at a proton frequency of 400.13 MHz. The spectroscopic task was controlled by a HP xw-4600 workstation, and the spectral plotting was obtained using Bruker TOPSPIN 2.1. The following abbreviations have been used in the assignment of NMR peaks: s = singlet; d = doublet; t = triplet; m = multiplet; and br = broad. The proton/carbon highlighted in bold represents the proton under investigation. The difluorodeoxycytidine ring of GEM has been represented as dFdC while aromatic moiety is abbreviated as Ar. The matrix assisted laser desorption ionization (MALDI) mass spectroscopy was performed in order to determine the molecular mass of GEM-PEG-MTX using Bruker MALDI-TOF instrument. For MALDI-TOF analysis, 0.5 mg of each conjugate was dissolved into 1 mL of deionized water and spectra were recorded.

**Synthesis of MTX-PEG-COOH.** MTX-NHS ester and PEGylated MTX were synthesized using the same protocol described in our earlier reports.<sup>14,15,17</sup> Briefly, MTX-NHS ester (40 mg, 0.074 mmol) was dissolved in 2 mL of anhydrous DMSO. Pyridine (1 mL) was added to the resultant solution, following which NH<sub>2</sub>-PEG-COOH (300 mg, 1 mmol) dissolved in DMSO (0.5 mL) was added dropwise under vigorous stirring. After 12 h, the reaction mixture was filtered and the filtrate was poured dropwise into an ice-cold mixture of diethyl ether and acetone (5:1) under vigorous stirring condition. The resulting solid was separated by decantation and redissolved in dichloromethane (DCM). Unreacted MTX-NHS ester was removed from the PEGylated one via filtration.

The filtrate was concentrated and poured dropwise into a mixture of ice-cold diethyl ether:acetone (10:1) to reprecipitate the MTX-PEG-COOH as a bright orange solid. The precipitate was isolated from the mother liquor via decantation, washed 3–4 times with cold ether to remove traces of DMSO, air-dried, and used for subsequent conjugation with GEM. State of aggregation: Yellow solid; Yield: 81.5%; FTIR ( $\nu_{\max}$ , KBr pellets  $\text{cm}^{-1}$ ): 3500–3200 (br,  $-\text{OH}$ ,  $\text{NHCO}$ ), 3100–2800 (br, aromatic  $\text{C}=\text{C}$ ,  $-\text{C}-\text{C}$ ), 1725 ( $-\text{COOH}$ ), 1629 ( $\text{CO}-\text{NH}$ , amide I), 1590 ( $\text{CO}-\text{NH}$ , amide II), 1467 ( $-\text{NH}_2$ ), 1343 ( $-\text{C}-\text{H}$ ), 1281, 1242 ( $-\text{C}-\text{O}-\text{C}$ ), 1114, 962, 841 ( $-\text{C}-\text{C}$ ,  $-\text{C}-\text{N}$ ).  $^1\text{H}$  NMR ( $\delta$ ,  $\text{DMSO}-d_6$ , ppm): 8.7 (s,  $\text{PtC}_7\text{H}$ , 1H), 8.1–7.9 (br m,  $-\text{PhCONHCH}$  overlapped with  $-\text{CONHCH}_2\text{CH}_2\text{PEG}-$ , 4H), 7.8–7.6 (d,  $\text{PhC}_2\text{H}$  and  $\text{Ph}-\text{C}_6\text{H}$ , 2H), 6.9 (br, s,  $\text{Pt}-\text{NH}_2$ , 2H), 6.7–6.6 (d,  $\text{PhC}_3\text{H}$  and  $\text{Ph}-\text{C}_5\text{H}$ , 2H), 4.5–4.4 (d,  $\text{PtC}_6\text{CH}_2$ , 2H), 3.8–3.4 (b,  $-\text{OCH}_2\text{CH}_2$  overlapped with  $-\text{CH}_2-\text{CCH}$ ), 3.1 (t,  $-\text{CONH}-\text{CH}_2\text{CCH}$ , 1H), 2.5 (s,  $-\text{CONH}-\text{CH}_2\text{CCH}$ , 1H), 2.5 (br s,  $-\text{OH}$ , 1H), 2.3 (m,  $-\text{CH}_2\text{CO}_2\text{H}$ , 2H), 2.1–1.9 (m,  $-\text{CHCH}_2\text{CH}_2$ , 1H), 1.8–1.7 (m,  $-\text{CHCH}_2\text{CH}_2$ , 1H). Mass (MALDI-TOF, EI):  $m/z$  3955 ( $\text{M}^+$ ).

**Synthesis of GEM-PEG-MTX.** MTX-PEG-COOH (100 mg, 0.051 mmol) was dissolved in a 1:1 (v/v) mixture of DMF/pyridine (5 mL) and activated with DCC (10.5 mg, 0.051 mmol) and NHS (5.86 mg, 0.051 mmol) using standard carbodiimide chemistry. Following activation for 4 h, an approximately 3-fold molar excess of GEM-hydrochloride salt (45.88 mg, dissolved in pyridine) was added to the activated mixture and left stirring for an additional 24 h. Subsequently, the reaction mixture was filtered to remove the precipitated DCU and the filtrate was poured dropwise to ice cold ether to facilitate the precipitation of GEM-PEG-MTX conjugate. The crude GEM-PEG-MTX conjugate was further dissolved in DCM to precipitate out excess, unreacted GEM. The precipitate was removed via filtration and the filtrate was reprecipitated with ether to isolate pure GEM-PEG-MTX. State of aggregation: Yellow solid; Yield: 78.2%; UV vis ( $\lambda_{\max}$ , nm): 262.5, 256.5. FTIR ( $\nu_{\max}$ , KBr pellets  $\text{cm}^{-1}$ ): 3500–3200 (br,  $-\text{OH}$ ,  $\text{NHCO}$ ), 3100–2800 (br, aromatic  $\text{C}=\text{C}$ ,  $-\text{C}-\text{C}$ ), 1642 ( $\text{CO}-\text{NH}$ , amide I), 1468 ( $-\text{NH}_2$ ), 1344 ( $-\text{C}-\text{H}$ ), 1281, 1243 ( $-\text{C}-\text{O}-\text{C}$ ), 1114, 962, 841 ( $-\text{C}-\text{C}$ ,  $-\text{C}-\text{N}$ ) (d,  $\text{Ph}-\text{C}_3\text{H}$  and  $\text{Ph}-\text{C}_5\text{H}$ , 2H).  $^1\text{H}$  NMR ( $\delta$ ,  $\text{DMSO}-d_6$ , ppm): 8.7 (s,  $\text{PtC}_7\text{H}$ , 1H), 7.9–7.8 (d,  $\text{dFdC}-\text{C}_2\text{H}$ , 1H), 7.7–7.6 (d,  $\text{PtC}_6-\text{CH}_2\text{NH}-\text{Ph}$  1H) 7.5–7.4 (d,  $\text{PhC}_2\text{H}$ , 1H) 7.4–7.3 (d,  $\text{Ph}-\text{C}_6\text{H}$ , 1H), 6.8–6.7 (d,  $\text{PhC}_3\text{H}$ , 1H), 6.6–6.5 (d,  $\text{Ph}-\text{C}_5\text{H}$ , 2H), 6.3–6.2 (m,  $\text{dFdC}-\text{C}_5\text{H}$ , 2H), 5.9–5.8 (d,  $\text{dFdC}-\text{C}_6\text{H}$ , 1H), 4.5–4.4 (d,  $\text{PtC}_6\text{CH}_2$ , 2H), 4.1–3.4 (b,  $-\text{OCH}_2\text{CH}_2$  overlapped with  $-\text{CH}_2-\text{CCH@FA}$  and  $\text{dFdC}-\text{C}_1\text{H}$ ,  $\text{C}_3\text{H}$ ,  $\text{C}_5\text{H}$ ), 3.1 (t,  $-\text{CONH}-\text{CH}_2\text{CCH}$ , 1H), 2.5 (s,  $-\text{CONH}-\text{CH}_2\text{CCH}$ , 1H), 2.5 (br s,  $-\text{OH}$ , 1H), 2.3 (m,  $-\text{CH}_2\text{CO}_2\text{H}$ , 2H), 2.1–1.9 (m,  $-\text{CHCH}_2\text{CH}_2$ , 1H overlapped with  $\text{dFdC}-\text{C}_4\text{H}$ ), 1.8–1.7 (m,  $-\text{CHCH}_2\text{CH}_2$ , 1H). Mass (MALDI-TOF, ES $^+$ ):  $m/z$  4174 ( $\text{M}^+$ ).

**Physico-Chemical Characterization of Synthesized Bioconjugate (GEM-PEG-MTX).** *Melting Temperature.* The melting temperature of conjugates/free drug was determined using melting point apparatus and revalidated using differential scanning calorimetry (DSC; Perkin-Elmer MicroDSC) was used to determine the melting point of bioconjugate. The instrument was calibrated for temperature and heat flow accuracy by using melting of pure indium (MP 156.6 °C and  $\Delta H$  of 25.45 J  $\text{g}^{-1}$ ). Sample was placed on nonhermetic aluminum pan and analyzed at temperature range

of 20–180 °C at a rate of 10 °C/min with nitrogen flow rate at 50 mL/min.<sup>16</sup>

**Solubility.** Samples were added in excess quantity in double distilled water and incubated at 37 °C for 24 h with gentle shaking at 80 rpm in a shaker bath. Following incubation the samples were centrifuged (13 000 rpm for 5 min) and supernatant collected and analyzed using UV spectrophotometer (Shimadzu UV 1800).<sup>18</sup>

**In Vitro Hydrolysis in Simulated Media.** The rate of GEM release in phosphate buffered saline (PBS) (pH 5.0 and pH 7.4) was used as a predictor to determine the hydrolytic stability of the conjugate in simulated media.<sup>8,19,20</sup> In addition to pH, the effect of crude protease on *in vitro* hydrolysis was also evaluated. Briefly, individual components/conjugate (100  $\mu\text{g}/\text{mL}$ ) was added to the media; aliquots were withdrawn at predetermined time intervals and analyzed by HPLC to quantify the amount of GEM released.

**In Vitro Drug Release in Plasma.** *In vitro* release of GEM from conjugate was evaluated by creating the degradation profile of the conjugate in the presence of rat plasma. Unmodified GEM and its degradation product 2',2'-difluorodeoxyuridine (dFdU) were measured by incubating free GEM and GEM-PEG-MTX conjugate in plasma (pH 7.4) for 24 h. Samples were withdrawn at predetermined time intervals and analyzed by validated bioanalytical method using HPLC.<sup>21</sup>

**In vitro Cytotoxicity Assay.** The cytotoxicity of synthesized conjugate, native bioactives, and their PEGylated forms were assayed colorimetrically by using MTT assay<sup>22</sup> in human breast adenocarcinoma cells (MCF-7; ATCC, Manassas, VA, USA). Briefly, the cells were grown in tissue culture flasks (75  $\text{cm}^2$ ) and maintained under 5%  $\text{CO}_2$  atmosphere at 37 °C. Minimum Essential Medium Eagle (MEM, Sigma) supplemented with Earle's salts, L-glutamine, nonessential amino acids, sodium bicarbonate, sodium pyruvate, 10% FBS, 100 U/mL penicillin, and 100  $\mu\text{g}/\text{mL}$  streptomycin (PAA Laboratories GmbH, Austria) was used as growth medium and changed on alternate days. The cells were harvested by a 0.25% w/v trypsin–EDTA solution (Sigma, USA) once 90% confluency was achieved and subcultured in 96-well culture plate (Costars, Corning Inc., NY, USA) at a density of 10 000 cells/well. Once the cells reached confluency, culture medium was removed and cells were washed thrice with Hank's Buffered Salt (HBS) Solution (PAA Laboratories GmbH, Austria). Following this, cells were incubated with different concentrations (0.001, 0.01, 0.1, and 1.0  $\mu\text{g}/\text{mL}$ ) of free drugs (GEM and MTX), physical mixture of drugs, PEGylated congeners, and synthesized conjugate (in equivalent concentrations of free GEM), and the extent of viability of the cells was evaluated by measuring the optical density at 540 nm spectrophotometrically.

**In Vivo Antitumor Efficacy.** Female Sprague–Dawley (SD) rats (180–200 g) were used to determine the antitumor potential of the synthesized conjugates. All animal study protocols were approved by the Institutional Animal Ethics Committee (IAEC) of National Institute of Pharmaceutical Education & Research (NIPER), SAS Nagar, India. All the experiments were performed in accordance with the guidelines of the Committee for the Purpose of Control and Supervision of Experiments on Animals (CPCSEA), India. Animals were housed in plastic cages having free access to food and water and kept under a 12 h light/dark cycle throughout the experimentation. A chemical-induced breast cancer model was used for the study and cancer was induced following our previously reported protocol.<sup>16,17,23,24</sup> Briefly, 7,12-dimethyl

benz[*a*]anthracene (DMBA) in soybean oil was administered at a dose of 45 mg/kg at weekly interval for three consecutive weeks. Measurable sized tumors were observed after 10 weeks of last dosing. Tumor bearing animals were divided randomly into different treatment groups comprising control (untreated group), free GEM, free MTX, a physical mixture of MTX and GEM, and GEM-PEG-MTX. Two additional subgroups comprised of animals treated with GEM-PEG and MTX-PEG were also included in order to determine the advantage of dual drug conjugate over the PEGylation of individual drug molecules. Each group ( $n = 8$ ) was intravenously injected with three repeated doses (on 0, 4, and 8 day) of corresponding formulation at a dose/dose equivalent to 5 mg/kg.<sup>12</sup> The tumor dimensions were measured using digital calipers up to 20 days. Additionally, behavioral changes and loss in body weight were routinely monitored throughout the treatment course. Finally, survival of the animals was analyzed using the Kaplan–Meier survival plot.<sup>25</sup>

**In Vivo Hepato- and Nephrotoxicity.** Female Swiss mice (20–25 g) were used for the toxicity study. Animals were divided into different treatment groups, each containing six animals ( $n = 6$ ), and treated with free GEM (10 mg/kg), free MTX (10 mg/kg), GEM-PEG (dose equivalent to 10 mg/kg of free GEM), MTX-PEG (dose equivalent to 10 mg/kg of free MTX), physical mixture of MTX and GEM (10 mg/kg), and GEM-PEG-MTX (dose equivalent to 10 mg/kg of free GEM) by single dose of intravenous injection via tail vein. After 7 days, blood samples were collected and analyzed for the levels of biochemical markers, viz., aspartate transaminase (AST) and alanine transaminase (ALT) for hepatotoxicity and blood urea nitrogen (BUN) and plasma creatinine level for nephrotoxicity by using commercially available kits (Accurex, Biomedical Pvt. Ltd.). Malondialdehyde (MDA) level was also estimated in liver tissue homogenate following our previously reported protocols.<sup>26</sup>

**Statistical Analysis.** All data unless otherwise specified are expressed as mean  $\pm$  SD. Statistical analysis was performed with Graph Pad Prism software (v 4.03, USA) using one-way ANOVA, followed by Tukey–Kramer multiple comparison test.  $P < 0.05$  was considered statistically significant.

## RESULTS AND DISCUSSION

**Synthesis and Spectral Characterization of Target Conjugate.** The precise objective of the present study was to enhance the therapeutic efficacy of intrinsically hydrophilic or hydrophobic drug molecules with inherently poor pharmacokinetic profiles. In line with that idea, a macromolecular bioconjugate was synthesized by combining GEM with MTX via an intermediary PEG spacer. The selection of MTX as second biological active molecule was based on its clinical acceptance for the treatment of a wide variety of tumors and relatively hydrophobic character, which was speculated to mitigate the extreme hydrophilicity of GEM by rendering the necessary hydrophilic–lipophilic balance. In line with our hypothesis, we sought to interlink GEM, PEG, and MTX via amide linkages as these bonds are chemoenzymatically more stable than their acetal, ketal, ester, imine, or hydrazone counterparts. As outlined in the Introduction, GEM rapidly metabolizes to dFdU in the presence of deoxycytidine deaminase, which is principally present in blood, liver, and kidney. In this perspective, amide bond formation was believed to supplement a useful tool for improving the stability of GEM against enzymatic degradation.

In the FTIR spectrum of MTX-NHS ester, a broad band centered around  $1600\text{ cm}^{-1}$  was documented. Following PEGylation, this band shifted to  $1642\text{ cm}^{-1}$ . Additional bands were observed within the range of  $1400\text{--}1800\text{ cm}^{-1}$  representing (i) free  $\alpha$ -carboxyl groups native to the structure of MTX; (ii) free carboxyl terminus of MTX-PEG conjugate; and (iii) multiple amide linkages interlinking MTX, PEG, as well as those native to the structure of MTX. In addition to the specified changes, an intense vibration was documented at  $1113\text{ cm}^{-1}$ . This band represented the  $\text{C-O}$  and  $\text{C-N}$  stretching vibrations of PEG. GEM-PEG-MTX conjugate presented an inherent broadening, particularly over the range of  $1400\text{--}1800\text{ cm}^{-1}$ , which was attributed to the superimposition of multiple amide I, amide II, carboxyl, and amine ( $\text{-NH}$ ) bending vibrations in the same region (Figure 2). The  $^1\text{H}$  proton NMR

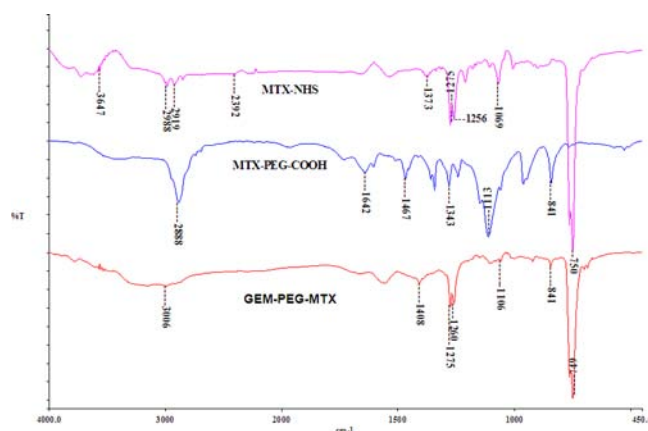


**Figure 2.** FTIR spectra of MTX-NHS, MTX-PEG-NHS, and GEM-PEG-MTX.

spectrum of the GEM-PEG-MTX conjugate compared to MTX-PEG and MTX-NHS ester has been depicted in Figure 3a. The detailed structural assignment has been shown in Figure 3. The final confirmation regarding structure came from MALDI-mass spectroscopy. The MALDI mass spectra of GEM-PEG-MTX compared with MTX-PEG has been depicted in Figure 4. In the case of MTX-PEG, the center of the bell was

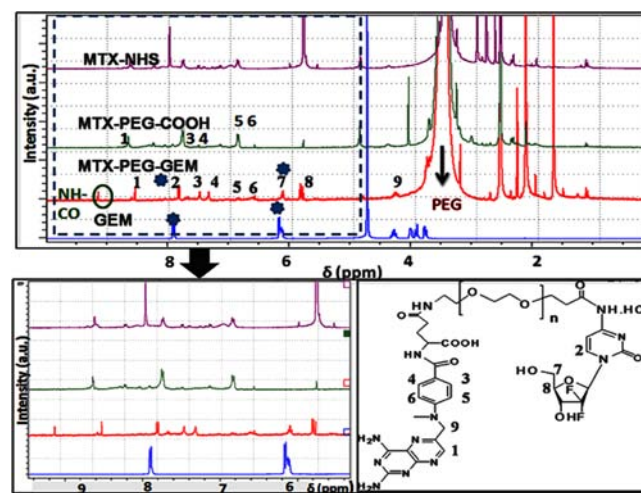


**Figure 3.**  $^1\text{H}$  NMR spectra of (a) MTX-NHS, MTX-PEG-NHS, GEM-PEG-MTX, and GEM. (b) Expanded view of aromatic region (c). Structural assignment of GEM-PEG-MTX.

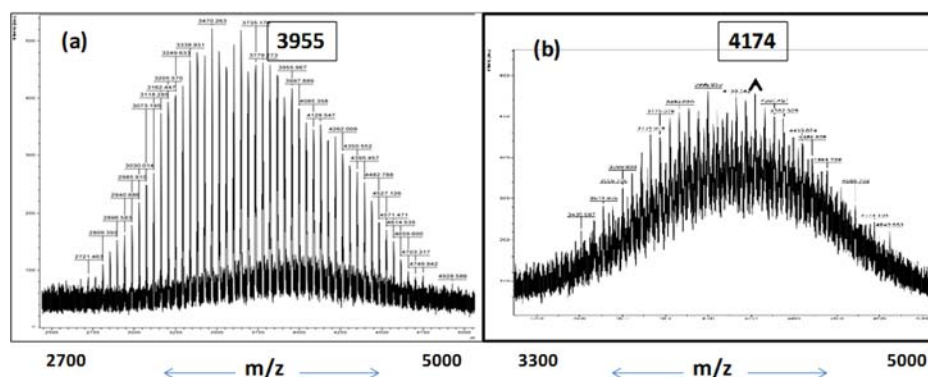


**Figure 4.** MALDI TOF-Mass spectra of (a) MTX-PEG-COOH (b) GEM-PEG-MTX.

observed at  $m/z$  3955, which was close to the molecular ion peak of the conjugate. After conjugation with GEM, the center of the bell shifted to  $m/z$  4174, which was very close to molecular ion peak of GEM-PEG-MTX conjugate.

**Physicochemical Properties of the Conjugate. Melting Temperature.** Melting temperatures of synthesized conjugate in comparison to individual components are shown in Table 1.

**Table 1. Melting Point of Developed Conjugates and Individual Native Bioactives**

samples	melting point ( $^{\circ}\text{C}$ )
GEM	$290 \pm 3^a$
MTX	$185 \pm 4^a$
GEM-PEG-MTX	42–44

<sup>a</sup>MP determined using melting point apparatus and DSC.

Melting temperature of the conjugate was found to be markedly different from either GEM or MTX. It was interesting to observe that melting point of the finally synthesized conjugate was found to be in the range of 42–44  $^{\circ}\text{C}$ , which is quite similar to that of PEG. The observed thermal behavior is easily interpretable by the relative proportion (%w/w) of the individual components in the synthesized conjugate. In the synthesized conjugates, PEG comprises of approximately 75–80% of the total mass of the conjugate; therefore, the physical properties of the conjugate was dominated by PEG.

**Solubility.** Hydrophilic–lipophilic balance of the conjugate was evaluated by determining aqueous solubility of GEM-bioconjugate in comparison with individual constituents. Table 2 presents the solubility profile of synthesized conjugate compared to free drug. The solubility of free GEM and GEM-PEG-MTX was found to be 75.05 mg/mL and 63.82 mg/mL, respectively, at 25  $^{\circ}\text{C}$ . Interestingly, conjugation of MTX with GEM using macromolecular PEG spacer led to marked changes

**Table 2. Solubility of Bioconjugate and Individual Constituents**

samples	solubility in water (mg/mL)
GEM-PEG-MTX	$63.82 \pm 4.88$
GEM-PEG	$85.43 \pm 0.36$
MTX-PEG	$36.54 \pm 5.46$
GEM	$75.05 \pm 4.23$
MTX	$0.1^a$

<sup>a</sup>Solubility measured in plain water.

in the solubility of both GEM and MTX. While pristine MTX presents very low solubility in water, the synthesized conjugate was freely soluble in water. This observation could be attributed to the presence of PEG spacer, which constitutes almost 80% of the synthesized conjugate. The results clearly indicate that appropriate molecular engineering can be used to transform the physicochemical properties of pharmaceutically active compounds which in turn can play a crucial role in pharmacological activity. Furthermore, the present strategy can be explored to fine-tune the pharmacokinetics and -dynamics of clinically established drugs with recognized problems.

**In Vitro Hydrolysis in Simulated Media.** The hydrolytic stability of the synthesized conjugate was assessed in simulated media in the absence and presence of proteases. As evident from Figure 5, a nominal amount of GEM was released at pH 5.5; the release, however, was slightly augmented at pH 7.4. This observation is in line with earlier reports.<sup>8,19,20</sup> Interestingly, addition of crude protease hardly influenced the rate of GEM release. Such an observation is not against streamline and may be attributed to experimental limitations that avert exact simulation of the actual tumor microenvironment under *in vitro* conditions.

**In Vitro GEM Release in Plasma.** It is well reported that free GEM converts to its metabolite 2',2'-difluorodeoxyuridine (dFdU) when exposed to plasma conditions. Therefore, it is of utmost importance that the synthesized conjugate provide the necessary stability against this enzymatic degradation. To verify the protective potential of the synthesized conjugate, both GEM-PEG-MTX and free GEM were incubated in plasma and a profile was created between the % GEM remaining and its metabolite (dFdU) with respect to time (Figure 6). *In vitro* plasma stability study demonstrated rapid degradation of free GEM, as evident by very high dFdU concentration (61% in 24 h). In the case of free GEM, only 39% of the parent drug was detected, following 24 h incubation in plasma. In contrast, GEM-PEG-MTX demonstrated controlled release over the 24 h, as only 20% of GEM was observed in plasma after 24 h. In fact, for the dual drug conjugate, only 13% of dFdU was detected in solution after 24 h postincubation, which was almost five times lower as compared to dFdU observed in the case of free GEM. The observation strongly supported the ability of synthesized conjugate in providing stability to GEM against deoxycytidine deaminase mediated degradation in plasma. The total amount of GEM released (sum of GEM and dFdU) from the conjugate over the 24 h time period was approximately 32%. This observation demonstrated that almost 70% of the GEM was still bound to the conjugate, while the

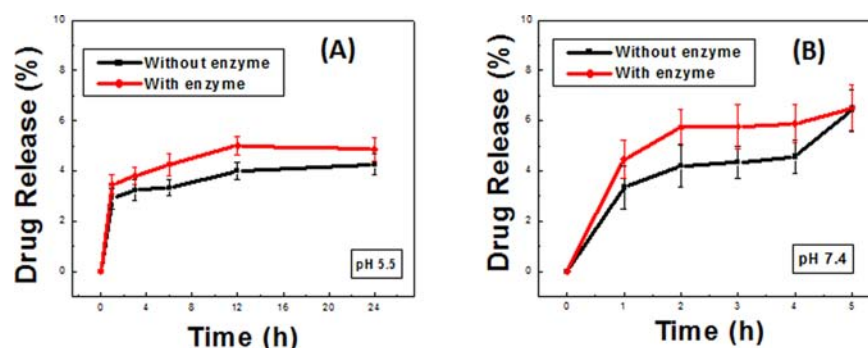


**Figure 5.** *In vitro* release of GEM-PEG-MTX at pH (A) 5.5 and (B) 7.4.

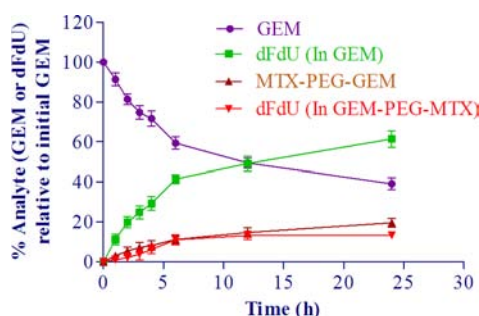


**Figure 6.** Time-dependent concentration of GEM and dFdU following incubation of free GEM and GEM-PEG-MTX in the presence of plasma.

value was as small as 39% in the case of free GEM. Controlled release and protection from degradation observed in the case of synthesized conjugate could be attributed to the stability of amide bond formed during the conjugate synthesis. Our findings are also in line with the previous reports in which GEM conjugates have been reported to extend the plasma stability.<sup>27</sup>

**In Vitro Cytotoxicity Assay.** Standard MTT *in vitro* cytotoxicity assay was performed to measure the cytotoxicity of free drugs and/or combinations, PEGylated form of free drugs, and combinatorial conjugate thereof against MCF-7 cell line. Time and concentration dependent reduction in cellular viability was observed in all the tested compounds (Table 3). Interestingly, a slight decrease in the cell cytotoxicity of conjugates (PEGylated and combinatorial conjugates) at early time points was observed which could be attributed to the delayed release of bioactive as compared to that of parent

**Table 3.** IC<sub>50</sub> Values of Conjugates and Free Drugs

sample	IC <sub>50</sub> value (μg/mL)		
	24 h	48 h	72 h
GEM	0.294 ± 0.03	0.181 ± 0.02	0.064 ± 0.006
MTX	0.591 ± 0.11	0.316 ± 0.07	0.119 ± 0.05
GEM+MTX <sup>a</sup>	0.106 ± 0.04	0.072 ± 0.004	0.03 ± 0.007
GEM-PEG <sup>b</sup>	0.325 ± 0.06	0.194 ± 0.08	0.048 ± 0.009
MTX-PEG <sup>c</sup>	0.667 ± 0.13	0.212 ± 0.05	0.073 ± 0.002
GEM-PEG-MTX <sup>b</sup>	0.181 ± 0.02	0.100 ± 0.04	0.019 ± 0.001

<sup>a</sup>Concentrations ranging from 0.01 to 10 μg/mL of GEM and MTX were exposed to cells for cytotoxicity studies. <sup>b</sup>Concentrations equivalent to 0.01–10 μg/mL of GEM were exposed to cells. <sup>c</sup>Concentrations equivalent to 0.01–10 μg/mL of MTX were exposed to cells. Values expressed as Mean ± SD (*n* = 4).

compound. In contrast, at later time points, i.e., >72 h, a significant increase in the cell cytotoxicity of combinatorial conjugates, measured as a function of 1.57-fold reduction in the IC<sub>50</sub> value as compared to free drug combination, was observed. This could be attributed to increased uptake owing to hydrophilic lipophilic balance and improved stability of GEM. Furthermore, upon comparing the cell cytotoxicity of the developed bioconjugate in recovery mode (6 h exposure followed by 18 h recovery), 2.09-fold reduction in the IC<sub>50</sub> value of the GEM-PEG-MTX was noted as compared to that of free drug combination. The results were further confirmed by apoptosis studies, according to which, GEM-PEG-MTX showed a 2.44-fold increase in the apoptotic index as compared to that of free drug combination (Supporting Information Figure S1). Our *in vitro* results are in concordance with the earlier reports by Aryal et al. in which combinatorial conjugate of GEM and PTX exerted higher anticancer efficacy *in vitro*, when compared to either free GEM or free PTX. In addition, functional properties of PEG molecules such as P-gp inhibition and alternate cellular internalization mechanisms are also anticipated to contribute to the overall improved synergistic cytotoxicity potential of synthesized combinatorial conjugate.<sup>3,28</sup> Prominent toxicity was observed in the case of cells exposed to free GEM, while no significant reduction in cell viability was observed for cells treated with free PEG. By integrating two pharmaceutically active molecules to the distal ends of a PEG spacer, we have been able to enhance the efficacy of the conjugate molecule to a favorable extent. These results not only justify the merit of combinatorial conjugation strategy, but also suggest that the dual drug conjugate developed in the course of the study are effectively internalized by their cellular target, following which, the covalent bonds interconnecting bioactive(s) and polymeric spacer slowly hydrolyze in the intracellular milieu to exert desired cytotoxicity.

**In Vivo Tumor Growth Inhibition Studies.** Having studied the *in vitro* anticancer efficacy of the synthesized conjugate and controls, we proceeded to evaluate its antitumor efficacy *in vivo*. Figure 7 presents the antitumor efficacy of chemically (DMBA) breast cancer induced rats, treated with free GEM, free MTX, physical mixture of GEM and MTX, GEM-PEG, MTX-PEG, and GEM-PEG-MTX conjugate. Among all treatment groups, animals treated with GEM-PEG-MTX showed the highest antitumor efficacy, which was significantly higher in comparison to that of free GEM (*p* < 0.001), free MTX (*p* < 0.001), physical mixture of MTX and GEM (*p* < 0.001), GEM-PEG (*p* < 0.001), and MTX-PEG (*p* < 0.01). While antitumor activity of MTX-PEG or GEM-PEG was higher than that of their free drug counterparts, the effect

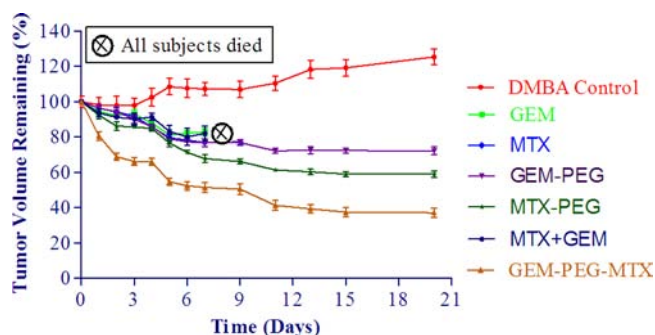


**Figure 7.** *In vivo* antitumor efficacy profile of GEM-PEG-MTX bioconjugate, free GEM, free MTX, physical mixture of MTX and GEM, GEM-PEG, and MTX-PEG. Plot indicates the percentage tumor volume remaining with time.

was significantly ( $p < 0.001$ ) lower as compared to GEM-PEG-MTX. These results revalidated that enhancement in anticancer efficacy was not only a consequence of PEGylation, but also a synergistic influence of dual drugs as well. Although significant reduction ( $p < 0.001$ ) in tumor volume was observed with free GEM, free MTX, or a physical mixture of MTX and GEM treated groups, acute drug-related toxicity was encountered in all these groups. In fact, animals treated with free GEM, free MTX, and a physical mixture of GEM and MTX died within 11 days after first dosing. While PEGylation of free drugs was able to alleviate the toxicity to some extent, side effects could not be completely eliminated. To further investigate the correlation of animal death due to severe drug-associated toxicity, a profile of body weight loss as a function of time was generated (Figure 8). A significant loss in body weight was observed in the case of

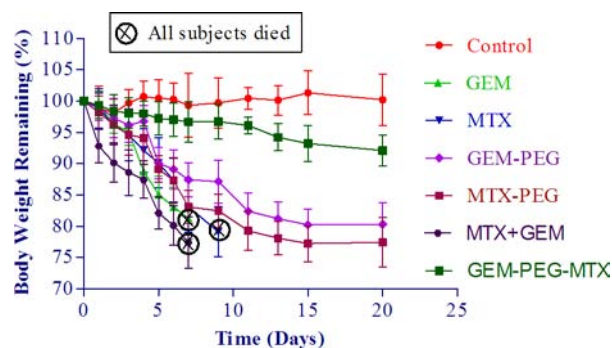


**Figure 8.** Decrease in body weight following administration of different formulations. Plot indicates the body weight remaining (%) with respect to time.

animals treated with free GEM, free MTX, a physical mixture of MTX and GEM, GEM-PEG, and MTX-PEG especially after second and third dosing. Animals treated with GEM, MTX, and their physical mixture became lethargic within a day of first intravenous dosing and were noticed to congregate at the corner of their cages. However, animals treated with GEM-PEG and MTX-PEG were in better physiological condition, suggesting lower toxicity of PEGylated conjugates over the free drugs. Interestingly, no significant weight loss was observed for animals treated with GEM-PEG-MTX. To further correlate the toxicity profile of the synthesized conjugates with animal death, a Kaplan–Meier survival analysis was done (Figure 9) which revealed 100% survival in the case of conjugate, while it was reduced to 50% in the case of PEGylated drugs (GEM-

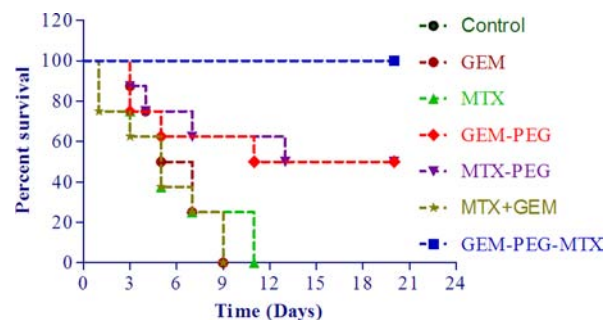


**Figure 9.** Kaplan–Meier survival analysis. Plot indicates the percent survival of animals with respect to time.

PEG and MTX-PEG). Survival rate reached 0% in the case of free GEM, free MTX, and physical mixture of MTX and GEM, as all the subjects died within 11 days after first dosing. Interestingly, no behavioral changes, viz., signs of labored breathing or difficulties in movement, were observed in animals treated with GEM-PEG-MTX. These results clearly indicated the superiority of GEM-PEG-MTX over other treatment groups. The observed enhancement in anticancer efficacy could be attributed to (i) higher intratumoral localization of the conjugate compared to free drug as a result of enhanced permeability and retention (EPR) effect facilitated by the stealth PEG linker and (ii) synergistic enhancement in anticancer efficacy endowed by the dual pharmacologically active molecules. Additionally, controlled and sustained release of active drugs over a protracted time period is believed to potentiate the effect of the synthesized conjugate at the pathological site, while alleviating side effects associated with high dose of single drugs.

***In Vivo* Hepato- And Nephrotoxicity.** Gemcitabine chemotherapy has been reported to cause cholestatic hepatotoxicity, nephrotoxicity, and hemolytic uremic syndrome.<sup>29,30</sup> Therefore, evaluation of hepatotoxicity and nephrotoxicity in the appropriate animal model was necessary to evaluate the safety potential of the developed conjugate. In addition to general toxicity monitoring in tumor-bearing rats, we also performed toxicity studies on Swiss mice, taking into consideration the better immunogenicity and immunosensitivity of mouse model in comparison to the rat one.<sup>24</sup> Liver is the principal site of accumulation and metabolism for most of the xenobiotics, and any enzyme level can be better correlated with the physiological state. Among the different biochemical markers, serum AST and ALT levels are important biochemical markers and their elevation directly reflects the hepatic injury. Figure 10 represents AST and ALT levels following the treatment with free drugs, PEGylated forms, and the developed conjugate. The group treated with GEM-PEG-MTX presented no significant change in comparison with control, suggesting hepatic safety potential of the developed conjugate. Notably, the AST levels in mice treated with free GEM (41.8 IU/L), free MTX (36.5 IU/L), physical mixture (43.6 IU/L), MTX-PEG (35.2 IU/L), and GEM-PEG (38.6 IU/L) were significantly higher than that of control. These results are in line with the previous reports in which GEM chemotherapy has been reported to cause mild to severe hepatotoxicity.<sup>30</sup> In contrast, normal levels of AST and ALT were observed in the case of GEM-PEG-MTX conjugate. These observations supported the conjugation strategy as an effective tool to synergize the therapeutic potential of individual drugs by alleviating the toxicity up to a reasonable extent. In line with the results of

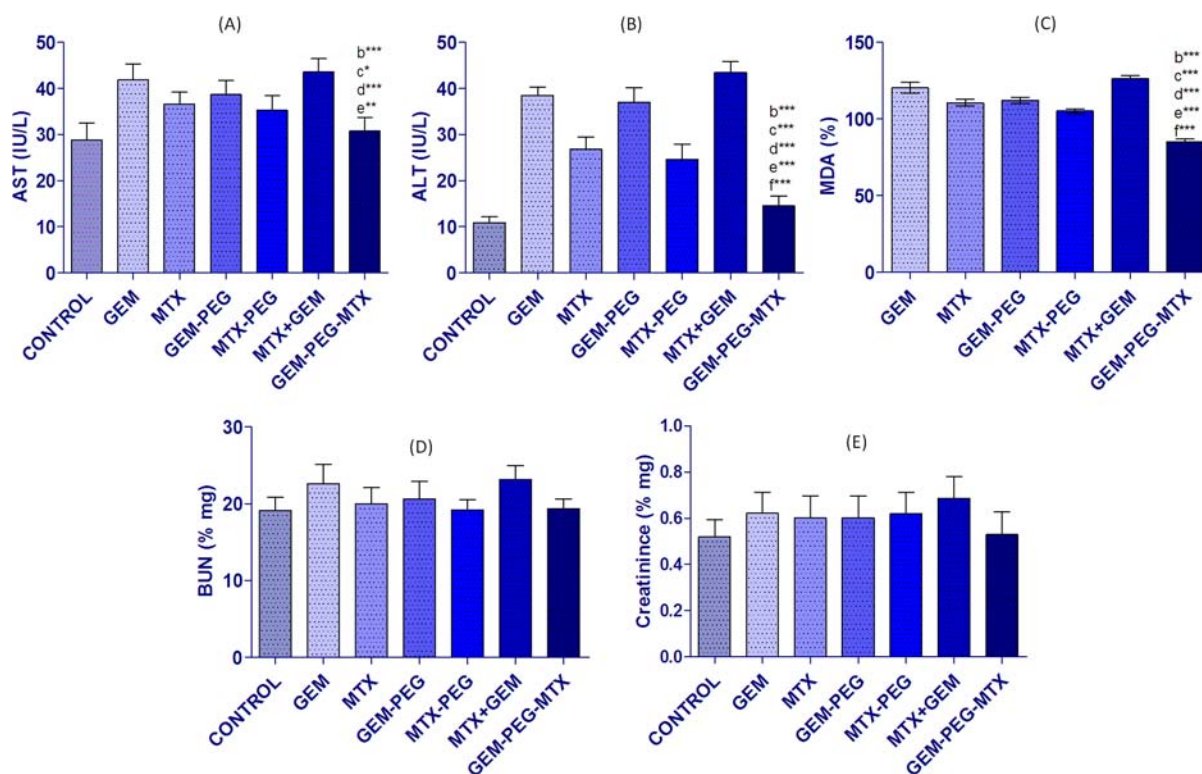


**Figure 10.** Biochemical markers (A) AST, (B) ALT, (D) BUN, (E) Creatinine levels in plasma and (C) MDA level in liver homogenate following administration of free GEM, free MTX, GEM-PEG, MTX-PEG, physical mixture of MTX and GEM, and GEM-PEG-MTX conjugate.

AST and ALT biochemical assays, conjugate treated animals presented insignificant difference in MDA level compared to control conjugates/free drugs indicating that GEM-PEG-MTX conjugate does not induce significant oxidative stress *in vivo*.

To further evaluate the nephrotoxicity of GEM-PEG-MTX conjugate, BUN and creatinine levels of mice treated with various formulations including free drug was estimated. Figure 10D,E summarizes the result of BUN and creatinine assays. Interestingly, none of the treatment groups exhibited nephrotoxicity as the difference in BUN and creatinine levels were insignificant in all the treatment groups. Although dose dependent and long-term toxicity need to be assessed to confirm the safety potential of the developed conjugate, yet the data in hand give an idea about the safety potential of the dual drug conjugate.

## CONCLUSION

In the present report, a dual drug macromolecular bioconjugate has been developed by combining MTX and GEM to the distal ends of a heterobifunctional PEG spacer. Given that the first article of combinatorial bioconjugation by Aryal et al. was limited to *in vitro* investigations, this is the first report which establishes the merits of the dual drug conjugation approach *in vivo*. In the course of extensive *in vitro* and *in vivo* studies, we have proven that combinatorial conjugation of MTX and GEM via hydrophilic and stealth PEG linker not only transformed the solubility profiles of constituent drug molecules, but also significantly improved their stability in simulated media and plasma. Tumor growth inhibition studies in chemically breast tumor induced rats clearly demonstrated the supremacy of the GEM-PEG-MTX conjugate over its free drug counterparts, PEGylated free drugs and physical mixture of free MTX and GEM. The result explicitly supported our hypothesis of

synergistic performance of dual drug conjugates over single drug or physical combination of two drugs. Our future studies will concentrate on evaluating the pharmacokinetic profile of GEM-PEG-MTX and correlate the findings with observed synergism.

## ASSOCIATED CONTENT

### Supporting Information

Results of apoptosis assay of developed bioconjugate against MCF-7 cells. This material is available free of charge via the Internet at <http://pubs.acs.org>.

## AUTHOR INFORMATION

### Corresponding Author

\*Telephone: 0172-2292055. Fax: 0172-2214692. E-mail: [sanyogjain@nipr.ac.in](mailto:sanyogjain@nipr.ac.in); [sanyogjain@rediffmail.com](mailto:sanyogjain@rediffmail.com).

### Author Contributions

Manasmita Das and Roopal Jain contributed equally.

### Notes

The authors declare no competing financial interest.

## ACKNOWLEDGMENTS

Authors are thankful to Director, NIPER, for providing necessary infrastructure facilities. M.D., A.K.A., and K.T. acknowledge the Department of Science and Technology (DST) and Council of Scientific and Industrial Research (CSIR), Government of India, for financial assistance. Technical assistance of Mr. Rahul Mahajan is duly acknowledged.

## REFERENCES

- (1) Martello, L. A.; McDaid, H. M.; Regl, D. L.; Yang, C. P. H.; Meng, D.; Pettus, T. R. R.; Kaufman, M. D.; Arimoto, H.; Danishefsky, S. J.,

- and Smith, A. B. (2000) Taxol and discodermolide represent a synergistic drug combination in human carcinoma cell lines. *Clin. Cancer Res.* 6, 1978–1987.
- (2) Tu, S. M., Hossan, E., Amato, R., Kilbourn, R., and Logothetis, C. J. (1995) Paclitaxel, cisplatin and methotrexate combination chemotherapy is active in the treatment of refractory urothelial malignancies. *J. Urol.* 154, 1719–1722.
- (3) Aryal, S., Hu, C. M. J., and Zhang, L. (2010) Combinatorial drug conjugation enables nanoparticle dual-drug delivery. *Small* 6, 1442–1448.
- (4) Xydakis, E., Repassos, E., Poulou, M., Papadakou, M., Boukis, C., and Panagos, G. (2006) Second line chemotherapy with methotrexate and gemcitabine in patients with relapsing head and neck cancer. *J. BUON.* 11, 419–424.
- (5) Kuribayashi, K., Miyata, S., Fukuoka, K., Murakami, A., Yamada, S., Tamura, K., Hirayama, N., Terada, T., Tabata, C., and Fujimori, Y. (2013) Methotrexate and gemcitabine combination chemotherapy for the treatment of malignant pleural mesothelioma. *Mol. Clin. Oncol.* 1, 639–642.
- (6) Reddy, L. H., and Couvreur, P. (2009) Squalene: A natural triterpene for use in disease management and therapy. *Adv. Drug Delivery Rev.* 61, 1412–1426.
- (7) Réjiba, S., Reddy, L. H., Bigand, C., Parmentier, C., Couvreur, P., and Hajri, A. (2011) Squalenoyl gemcitabine nanomedicine overcomes the low efficacy of gemcitabine therapy in pancreatic cancer. *Nanomedicine* 7, 841–849.
- (8) Pasut, G., Canal, F., Dalla Via, L., Arpicco, S., Veronese, F. M., and Schiavon, O. (2008) Antitumoral activity of PEG–gemcitabine prodrugs targeted by folic acid. *J. Controlled Release* 127, 239–248.
- (9) Chitkara, D., Mittal, A., Behrman, S. W., Kumar, N., and Mahato, R. I. (2013) Self-assembling, amphiphilic polymer-gemcitabine conjugate shows enhanced antitumor efficacy against human pancreatic adenocarcinoma. *Bioconjugate Chem.* 24, 1161–1173.
- (10) Chitkara, D., and Kumar, N. (2013) BSA-PLGA-based core-shell nanoparticles as carrier system for water-soluble drugs. *Pharm. Res.* 30, 2396–2409.
- (11) Aapro, M. S., Martin, C., and Hatty, S. (1998) Gemcitabine-a safety review. *Anticancer Drugs* 9, 191–202.
- (12) Reddy, L. H., Marque, P.-E., Dubernet, C., Mouelhi, S.-L., Desmaele, D., and Couvreur, P. (2008) Preclinical toxicology (subacute and acute) and efficacy of a new squalenoyl gemcitabine anticancer nanomedicine. *J. Pharmacol. Exp. Ther.* 325, 484–490.
- (13) Vandana, M., and Sahoo, S. K. (2010) Long circulation and cytotoxicity of PEGylated gemcitabine and its potential for the treatment of pancreatic cancer. *Biomaterials* 31, 9340–9356.
- (14) Das, M., Mishra, D., Dhak, P., Gupta, S., Maiti, T. K., Basak, A., and Pramanik, P. (2009) Biofunctionalized, phosphonate-grafted, ultrasmall iron oxide nanoparticles for combined targeted cancer therapy and multimodal imaging. *Small* 5, 2883–2893.
- (15) Jain, S., Mathur, R., Das, M., Swarnakar, N. K., and Mishra, A. K. (2011) Synthesis, pharmacoscintigraphic evaluation and antitumor efficacy of methotrexate-loaded, folate-conjugated, stealth albumin nanoparticles. *Nanomedicine* 6, 1733–1754.
- (16) Das, M., Datir, S. R., Singh, R. P., and Jain, S. (2013) Augmented anticancer activity of a targeted, intracellularly activatable, theranostic nanomedicine based on fluorescent and radiolabeled, methotrexate-folic acid-multiwalled carbon nanotube conjugate. *Mol. Pharmaceutics* 10, 2543–2557.
- (17) Das, M., Singh, R. P., Datir, S. R., and Jain, S. (2013) Intracellular drug delivery and effective in vivo cancer therapy via estradiol-PEG-appended multiwalled carbon nanotubes. *Mol. Pharmaceutics* 10, 3404–3416.
- (18) Rao, M., Mandage, Y., Thanki, K., and Bhise, S. (2010) Dissolution improvement of simvastatin by surface solid dispersion technology. *Dissolution Technol.* 17, 27–34.
- (19) Cavallaro, G., Mariano, L., Salmaso, S., Caliceti, P., and Gaetano, G. (2006) Folate-mediated targeting of polymeric conjugates of gemcitabine. *Int. J. Pharm.* 307, 258–269.
- (20) Immordino, M. L., Brusa, P., Rocco, F., Arpicco, S., Ceruti, M., and Cattel, L. (2004) Preparation, characterization, cytotoxicity and pharmacokinetics of liposomes containing lipophilic gemcitabine prodrugs. *J. Controlled Release* 100, 331–346.
- (21) Lin, N.-M., Zeng, S., Ma, S.-L., Fan, Y., Zhong, H.-J., and Fang, L. (2004) Determination of gemcitabine and its metabolite in human plasma using high-pressure liquid chromatography coupled with a diode array detector. *Acta Pharmacol. Sin.* 25, 1584–1589.
- (22) Jain, S., Kumar, S., Agrawal, A. K., Thanki, K., and Banerjee, U. C. (2013) Enhanced transfection efficiency and reduced cytotoxicity of novel lipid-polymer hybrid nanoplexes. *Mol. Pharmaceutics* 10, 2416–2425.
- (23) Jain, A. K., Swarnakar, N. K., Das, M., Godugu, C., Singh, R. P., Rao, P. R., and Jain, S. (2011) Augmented anticancer efficacy of doxorubicin-loaded polymeric nanoparticles after oral administration in a breast cancer induced animal model. *Mol. Pharmaceutics* 8, 1140–1151.
- (24) Jain, S., Patil, S. R., Swarnakar, N. K., and Agrawal, A. K. (2012) Oral delivery of doxorubicin using novel polyelectrolyte-stabilized liposomes (layersomes). *Mol. Pharmaceutics* 9, 2626–2635.
- (25) Jain, S., Kumar, D., Swarnakar, N. K., and Thanki, K. (2012) Polyelectrolyte stabilized multilayered liposomes for oral delivery of paclitaxel. *Biomaterials* 33, 6758–6768.
- (26) Jain, S., Valvi, P. U., Swarnakar, N. K., and Thanki, K. (2012) Gelatin coated hybrid lipid nanoparticles for oral delivery of amphotericin B. *Mol. Pharmaceutics* 9, 2542–53.
- (27) Kiew, L.-V., Cheong, S.-K., Sidik, K., and Chung, L.-Y. (2010) Improved plasma stability and sustained release profile of gemcitabine via polypeptide conjugation. *Int. J. Pharm.* 391, 212–220.
- (28) Thanki, K., Gangwal, R. P., Sangamwar, A. T., and Jain, S. (2013) Oral delivery of anticancer drugs: challenges and opportunities. *J. Controlled Release* 170, 15–40.
- (29) Brodowicz, T., Wiltshcke, C., Zielinski, C. C., and Breiteneder, S. (1997) Gemcitabine-induced hemolytic uremic syndrome: a case report. *J. Natl. Cancer Inst.* 89, 1895–1896.
- (30) Robinson, K., Lambiase, L., Li, J., Monteiro, C., and Schiff, M. (2003) Fatal cholestatic liver failure associated with gemcitabine therapy. *Dig. Dis. Sci.* 48, 1804–1808.